Anion sensing with a Lewis acidic BODIPY-antimony(V) derivative

A. M. Christianson[a] and F. P. Gabbaï[a]*
[a]Department of Chemistry, Texas A&M University, College Station, Texas 77843-3255, United States of America

Supplementary Information

Contents:

S1. Experimental Section

General Methods. All preparations were carried out under an N_2 atmosphere using standard Schlenk techniques unless otherwise stated. Solvents were dried by refluxing under N_2 over Na/K (Et_2O, THF); all other solvents were ACS reagent grade and used as received. Starting materials and reagents were purchased and used as received, except for Ph_2SbCl, which was synthesized according to literature procedures.[1] NMR spectra were recorded using a Varian Unity Inova 500 FT NMR (499.58 MHz for ^1H, 125.63 MHz for ^{13}C) spectrometer. Chemical shifts (δ) are given in ppm and are referenced against residual solvent signals. Elemental analyses were performed at Atlantic Microlab (Norcross, GA). Absorbance measurements were taken on a Shimadzu UV-2502PC UV-Vis spectrophotometer against a solvent reference. Fluorescence measurements were taken on samples in capped quartz cuvettes under air on a PTI QuantaMaster spectrofluorometer with entrance and exit slit widths of 2 nm. Quantum yield measurements were referenced against a value of 0.91 for fluorescein in 0.1 M NaOH.[2, 3]

Synthesis of 1-F_2. 1-F_2 was synthesized by a modification of literature procedures.[4] A solution of 2,4-dimethylpyrrole (1.49 g, 15.7 mmol) and *p*-bromobenzaldehyde (1.50 g, 8.1 mmol) in 100 mL CH_2Cl_2 was treated with 5 drops of trifluoroacetic acid. The resulting solution was allowed to stir overnight under N_2 at room temperature leading to a yellow solution. This solution was then treated with solid *p*-chloranil (1.94 g, 7.9 mmol), resulting in the formation of a precipitate and a color change to deep red. After stirring overnight under N_2, this solution was treated with neat NEt_3 (8 mL) and 10 minutes later, with neat $BF_3{\cdot}Et_2O$ (8 mL) which was added via syringe. These additions resulted in dark brown-black solution. This mixture was stirred for 6 h at room temperature, then quenched with 100 mL H_2O. The organic layer was extracted 3x with H_2O and once with brine, then dried over $MgSO_4$ and filtered through a pad of silica. The dark red filtrate was reduced and purified by flash chromatography on silica gel (gradient of 0-100% CH_2Cl_2 in hexanes). The first major fraction was evaporated and washed with pentane to yield **1**-F_2 as a bright red-orange powder. Yield: 550 mg (17%). ^1H NMR (499.58 MHz, $CDCl_3$: 7.26 ppm): δ 7.64 (d, 2, *J* = 8.4 Hz), 7.18 (d, 2, *J* = 8.4 Hz), 5.99 (s, 2), 2.55 (s, 6), 1.41 (s, 6). Spectral data are in accord with previous reports.[4]

Synthesis of 1-Me_2**.** A solution of **1**-F_2 (550 mg, 1.36 mmol) in 15 mL of dry toluene was treated under N_2 with trimethylaluminum (250 mg, 3.47 mmol) and stirred at room temperature for 30 minutes. The reaction was quenched with H_2O and the organic fraction separated, dried over $MgSO_4$, and filtered. The filtrate was evaporated and washed with pentane to yield the crude product as an orange powder. The product could be further purified by flash chromatography on silica gel (gradient of 0-100% CH_2Cl_2 in hexanes). The first major fraction yielded **1**-Me_2 as a bright orange crystalline solid. Yield: 505 mg (94%). ^1H NMR (499.58 MHz, $CDCl_3$: 7.26 ppm): δ 7.62 (d, 2, *J* = 8.4 Hz), 7.21 (d, 2, *J* = 8.4 Hz), 5.99 (s, 2), 2.48 (s, 6), 1.39 (s, 6), 0.26 (s,6). ^{13}C NMR (125.63 MHz, $CDCl_3$: 77.00 ppm), δ: 152.51 (s), 140.35 (s), 138.65 (s), 135.37 (s), 132.08 (s), 130.28 (s), 129.52 (s), 122.67 (s), 121.79 (s), 16.43 (s), 14.88 (m), 9.52 (br). Elemental Analysis Calculated for $C_{21}H_{24}BN_2Br$: C, 63.83; N, 7.09; H, 6.12. Found: C, 63.63; N, 6.94; H, 6.27.

Synthesis of 2. A solution of **1**-Me_2 (400 mg, 1.01 mmol) in 20 mL Et_2O was treated with *n*-butyllithium (0.45 mL, 2.65 M in hexanes, 1.19 mmol) dropwise at -78° C. Upon stirring, the solution was allowed warm to room temperature over a period of 45 minutes. It was then cooled back to -78° C at which point Ph_2SbCl (357 mg, 1.15 mmol) in 5 mL THF was added via cannula. The mixture was allowed to stir and warm to room temperature overnight. The reaction was quenched with 20 mL of H_2O and extracted with 3 successive 20-mL portions of ethyl acetate. The organic fraction was washed with brine, dried over $MgSO_4$, and filtered. The filtrate was reduced and purified by flash chromatography on silica gel, eluting as the second major fraction with 10% ethyl acetate in hexanes. The product was dried to yield **2** as an orange powder. Orange crystals suitable for X-ray diffraction were obtained by slow evaporation of a CH_2Cl_2:Et_2O solution. Yield: 158 mg (26%). ^{1}H NMR (499.58 MHz, $CDCl_3$: 7.26 ppm): δ 7.52 (d, 2, *J* = 7.9 Hz), 7.43 (m, 4), 7.35 (m, 6), 7.27 (d, 2, *J* = 7.9 Hz), 5.98 (s, 2), 2.48 (s, 6), 1.40 (s, 6), 0.26 (s,6). ^{13}C NMR (125.63 MHz, $CDCl_3$: 77.00 ppm), δ: 152.18 (s), 141.57 (s), 139.00 (s), 138.75 (s), 138.08 (s), 136.78 (s), 136.48 (s), 136.21 (s), 129.70 (s), 129.44 (s), 128.94 (s), 128.79 (s), 121.60 (s), 16.44 (s), 14.65 (s), 9.56 (br). Elemental Analysis Calculated for $C_{33}H_{34}BN_2Sb$: C, 67.04; N, 4.74; H, 5.80. Found: C, 67.16; N, 4.73; H, 5.95.

Synthesis of [3]OTf. 2 (110 mg, 0.19 mmol) and methyl triflate (135 mg, 0.82 mmol) were combined in 15 mL of dry CH_2Cl_2 under N_2 and the solution was refluxed at 50° C for 5 h. The resulting dark orange solution was reduced and purified by flash chromatography on silica gel, eluting as the second major fraction with 3% MeOH in CH_2Cl_2. The product was dried and reprecipitated with Et_2O to yield [**3**]OTf as an orange powder. Orange crystals suitable for X-ray diffraction were obtained by slow evaporation of a CH_2Cl_2:Et_2O solution. Yield: 56 mg (40%).^{1}H NMR (499.58 MHz, $CDCl_3$: 7.26 ppm): δ 7.77 (d, 2, *J* = 8.1 Hz), 7.65 (m, 6), 7.58 (m, 6), 6.00 (s, 2), 2.64 (s, 3), 2.49 (s, 6), 1.38 (s, 6), 0.26 (s, 6). ^{13}C NMR (125.63 MHz, $CDCl_3$: 77.00 ppm), δ: 152.98 (s), 141.38 (s), 139.11 (s), 138.42 (s), 135.13 (s), 135.05 (s), 132.91 (s), 130.73 (s), 130.52 (s), 129.22 (s), 126.21 (s), 125.29 (s), 122.10 (s), 118.94 (s), 16.47 (s), 14.81 (s), 9.40 (br), 5.21 (s). ^{19}F NMR (470.00 MHz $CDCl_3$, BF_3·Et_2O: -153.00 ppm), δ: -78.38 ppm. Elemental Analysis Calculated for $C_{35}H_{37}BF_3N_2O_3SSb$: C, 55.66; N, 3.71; H, 4.94. Found: C, 55.60; N, 3.77; H, 4.86.

Theoretical Methods. All computations were performed using the Gaussian 09 suite of programs.[5] Ground state optimization calculations for [**3**]$^+$, **3**-F, and **3**-CN were performed using the B3LYP functional, with the mixed basis set: Sb, aug-cc-pVTZ-PP; B/F, 6-31g(d'); C/H/N, 6-31g(d). Excited state optimization calculations for [**3**]$^+$ were also performed using the B3LYP functional, with the same mixed basis set. An acetonitrile solvent function using the polarizable continuum model was also applied for excited state calculations.

S2. NMR Spectra of Novel Compounds

Figure S1. 1-Me_2

^{1}H

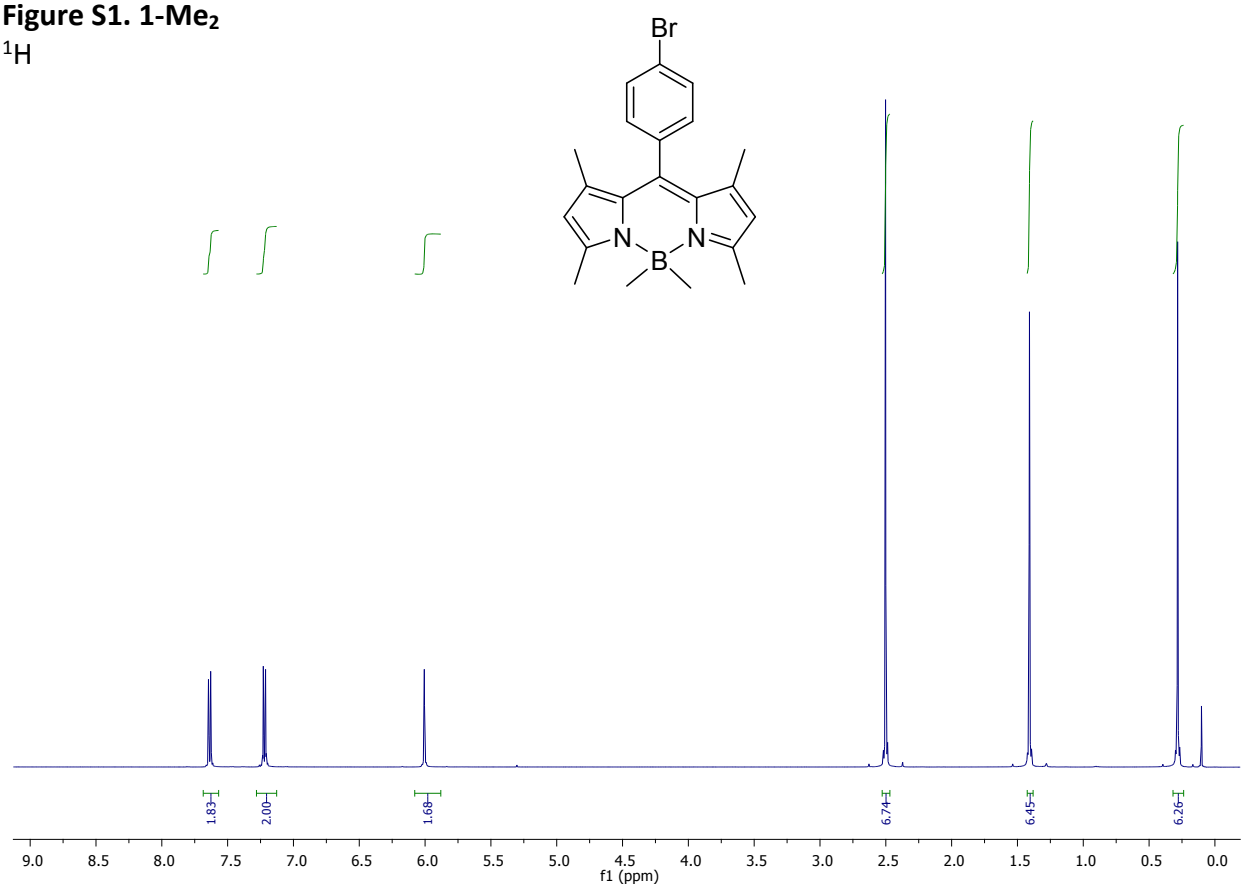

^{13}C

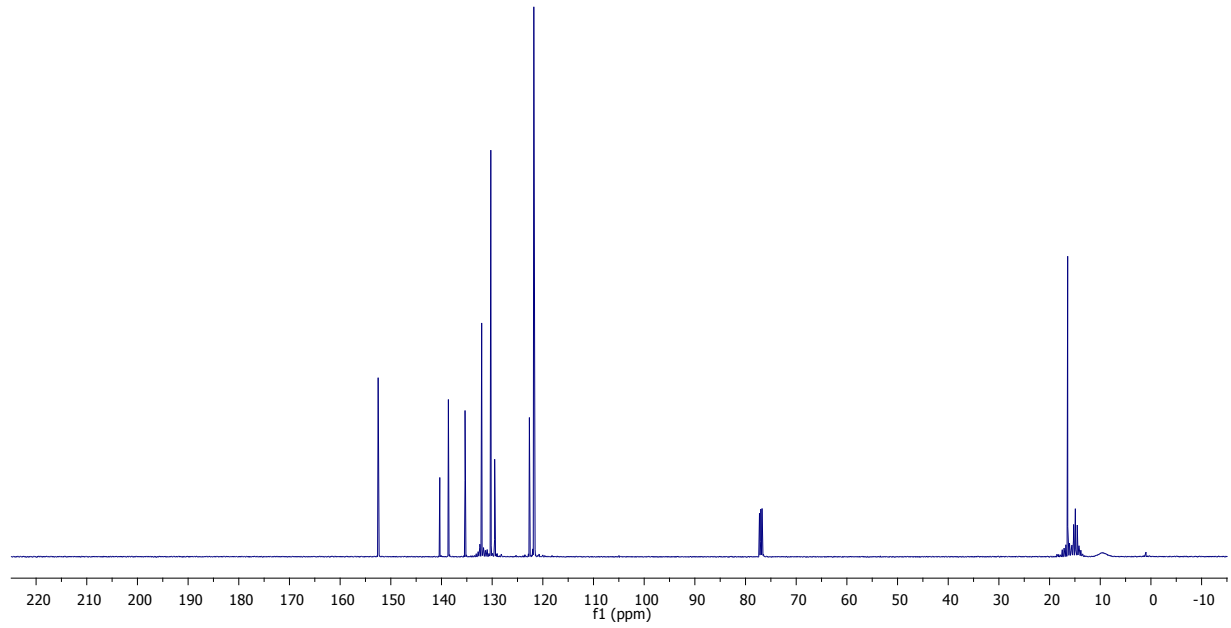

Figure S2. 2

^{1}H

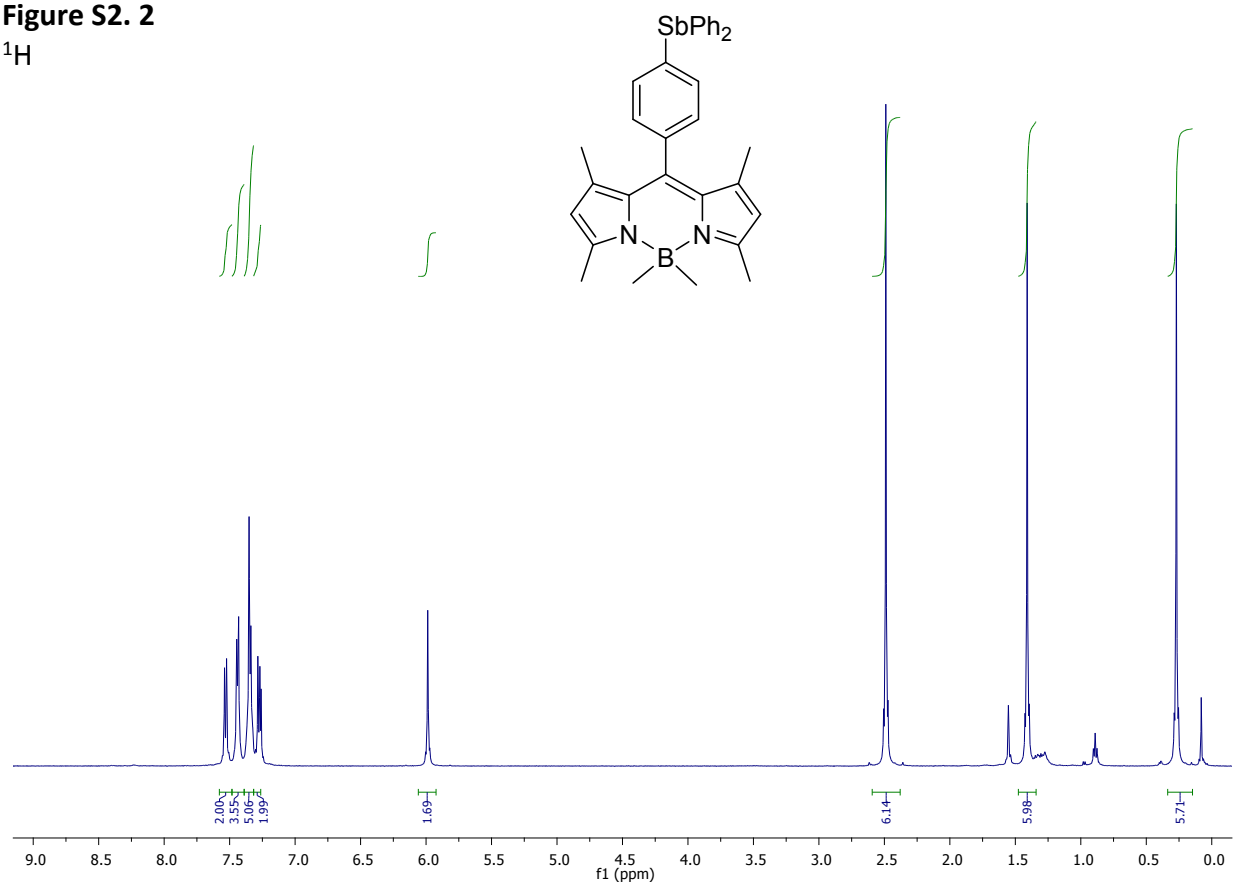

^{13}C

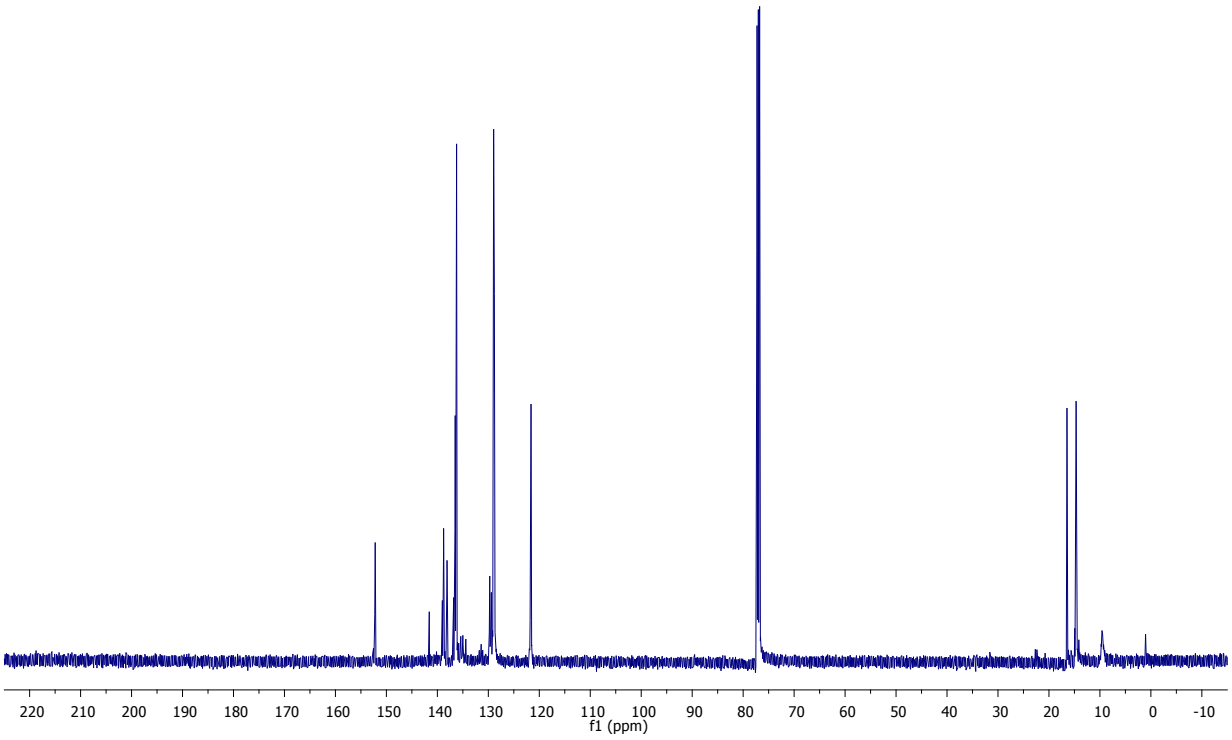

Figure S3. [3]OTf

^{1}H

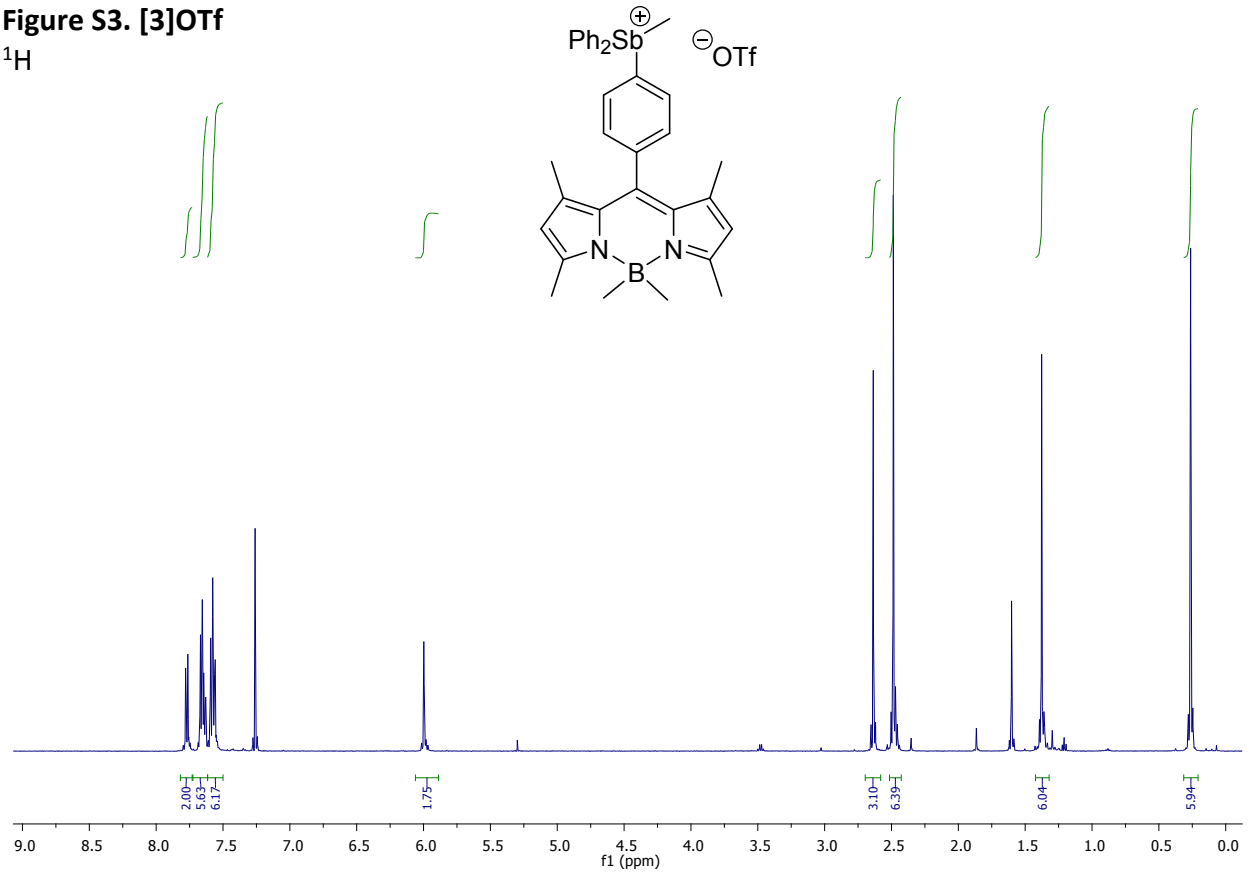

^{13}C

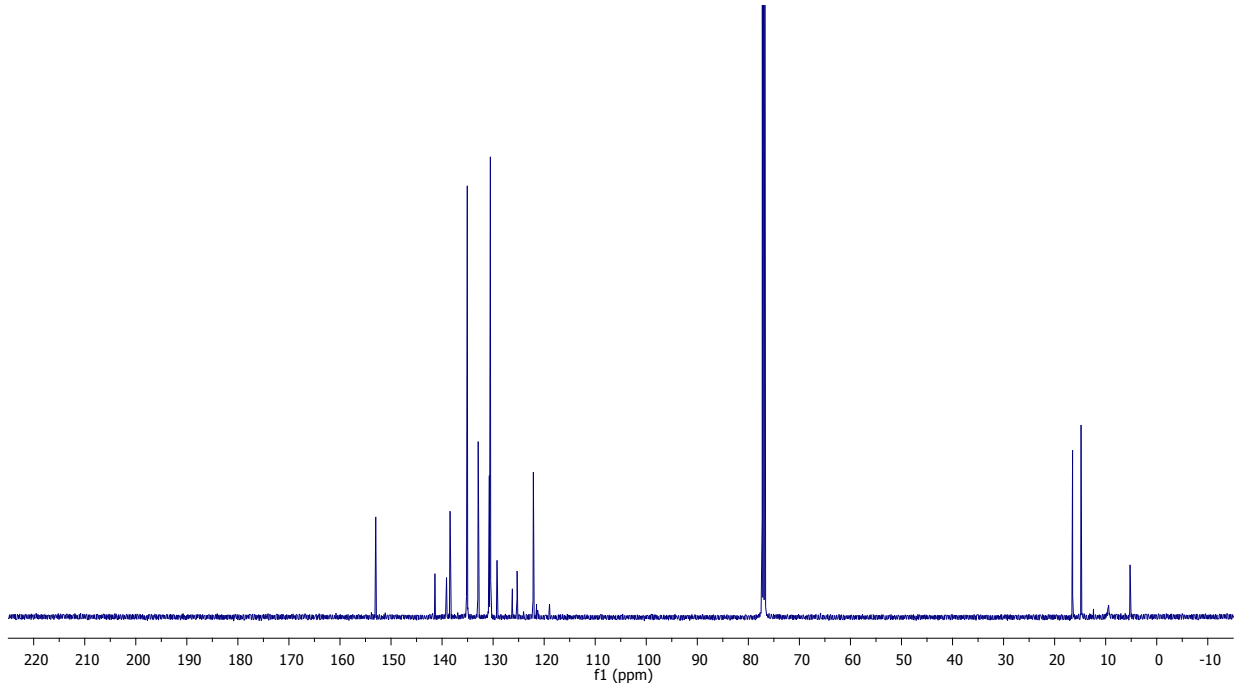

S3. Crystallographic Data for 2, [3]OTf, and 3-F

Figure S4. Crystal structure of **2**.

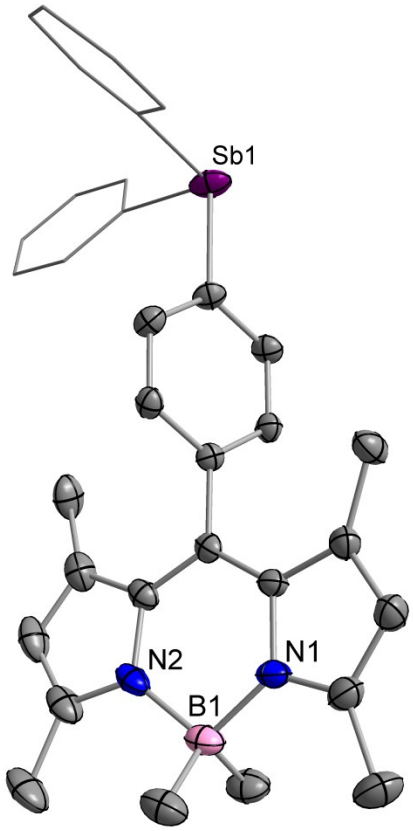

Table S1. Crystallographic details for **2**.

Chemical formula	$C_{33}H_{34}BN_2Sb$
M_r	591.18
Crystal system, space group	Monoclinic, *C*2/*c*
Temperature (K)	100
a, *b*, *c* (Å)	50.4025 (18), 11.0109 (4), 10.1952 (4)
β (°)	97.294 (1)
V (Å^3)	5612.3 (4)
Z	8
Radiation type	Mo *K*α
μ (mm^{-1})	1.01

Crystal size (mm)	0.20 × 0.11 × 0.04
Diffractometer	CCD area detector diffractometer
Absorption correction	Multi-scan *SADABS*
T_{min}, T_{max}	0.824, 0.961
No. of measured, independent and observed [$I > 2\sigma(I)$] reflections	60468, 6964, 4990
R_{int}	0.068
$(\sin \theta/\lambda)_{max}$ (Å^{-1})	0.668
$R[F^2 > 2\sigma(F^2)]$, $wR(F^2)$, S	0.052, 0.124, 1.08
No. of reflections	6964
No. of parameters	383
No. of restraints	4
H-atom treatment	H-atom parameters constrained
	$w = 1/[\sigma^2(F_o^2) + (0.0428P)^2 + 29.5865P]$ where $P = (F_o^2 + 2F_c^2)/3$
$\Delta\rho_{max}$, $\Delta\rho_{min}$ (e Å^{-3})	2.51, −2.40

Table S2. Crystallographic details for [**3**]OTf.

Chemical formula	$C_{34}H_{37}BN_2Sb\cdot(CF_3O_3S)$
M_r	755.29
Crystal system, space group	Monoclinic, $P2_1/c$
Temperature (K)	100
a, b, c (Å)	13.6694 (6), 24.9626 (12), 10.0894 (5)
β (°)	94.504 (2)
V (Å^3)	3432.1 (3)
Z	4
Radiation type	Mo $K\alpha$
μ (mm^{-1})	0.92
Crystal size (mm)	0.37 × 0.18 × 0.03
Diffractometer	CCD area detector

	diffractometer
Absorption correction	Multi-scan *SADABS*
T_{min}, T_{max}	0.728, 0.973
No. of measured, independent and observed [$I > 2\sigma(I)$] reflections	99924, 7050, 5899
R_{int}	0.092
$(\sin \theta/\lambda)_{max}$ (Å^{-1})	0.626
$R[F^2 > 2\sigma(F^2)]$, $wR(F^2)$, S	0.044, 0.096, 1.12
No. of reflections	7050
No. of parameters	422
H-atom treatment	H-atom parameters constrained
$\Delta\rho_{max}$, $\Delta\rho_{min}$ (e Å^{-3})	2.68, −0.67

Table S3. Crystallographic details for [**3**]F.

Chemical formula	$C_{34}H_{37}BFN_2Sb\cdot(CH_4O)$
M_r	657.26
Crystal system, space group	Monoclinic, $P2_1/c$
Temperature (K)	163
a, b, c (Å)	12.917 (3), 23.857 (4), 10.1194 (18)
β (°)	92.282 (13)
V (Å^3)	3115.9 (10)
Z	4
Radiation type	Mo $K\alpha$
μ (mm^{-1})	0.92
Crystal size (mm)	0.52 × 0.02 × 0.02
Diffractometer	Bruker *APEX*-II CCD diffractometer
Absorption correction	Multi-scan *SADABS*
No. of measured, independent and	27085, 4881, 2792

observed [$I > 2\sigma(I)$] reflections	
R_{int}	0.196
θ_{max} (°)	24.0
$(\sin \theta/\lambda)_{max}$ (Å^{-1})	0.572
$R[F^2 > 2\sigma(F^2)]$, $wR(F^2)$, S	0.059, 0.149, 0.99
No. of reflections	4881
No. of parameters	380
H-atom treatment	H-atom parameters constrained
$\Delta\rho_{max}$, $\Delta\rho_{min}$ (e Å^{-3})	0.60, −1.06

S4. Absorption and Emission Spectra of 2 and [3]OTf

Absorption and emission spectra were recorded in dichloromethane. Emission spectra were obtained with λ_{exc} = 490 nm. Fluorescence quantum yields were calculated based on gradients of integrated emission (IE) versus absorbance at λ_{exc} (Abs) for a series of measurements on the sample and fluorescence standard (fluorescein), according to the following equation:[6]

$$\Phi_{sample} = \Phi_{std} \times \frac{IE_{sample}}{IE_{std}} \times \frac{Abs_{std}}{Abs_{sample}} \times \left(\frac{\eta_{sample}}{\eta_{std}}\right)^2 = \Phi_{std} \times \frac{Grad_{sample}}{Grad_{std}} \times \left(\frac{\eta_{sample}}{\eta_{std}}\right)^2$$

where η was taken as 1.33 for 0.1 M NaOH and as 1.424 for dichloromethane. The resulting gradient plots obtained are shown below for compounds **2** and [**3**]OTf.

Figure S5. a) Normalized absorption and emission spectra of **2**. **b)** Beer-Lambert absorbance plot. **c)** Quantum yield gradient plot.

a)

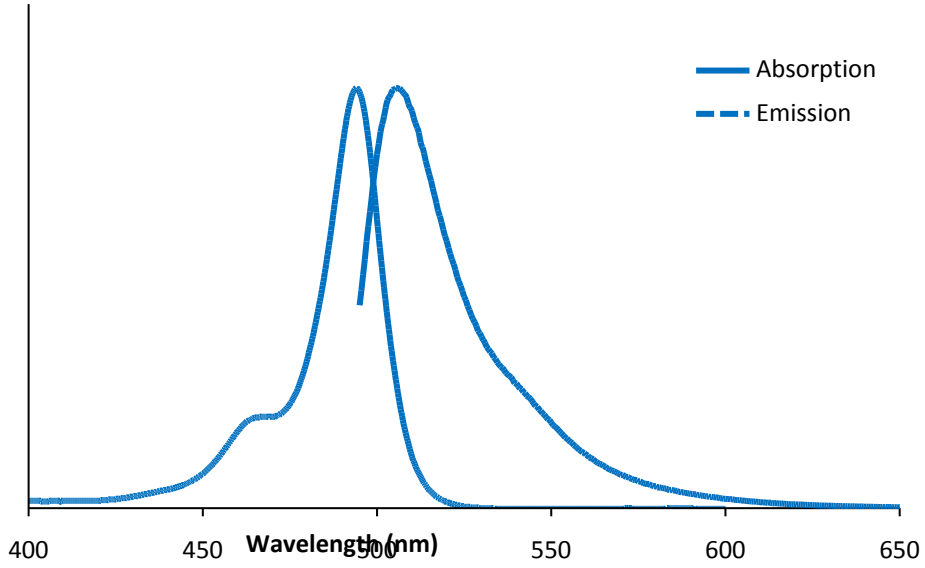

b)

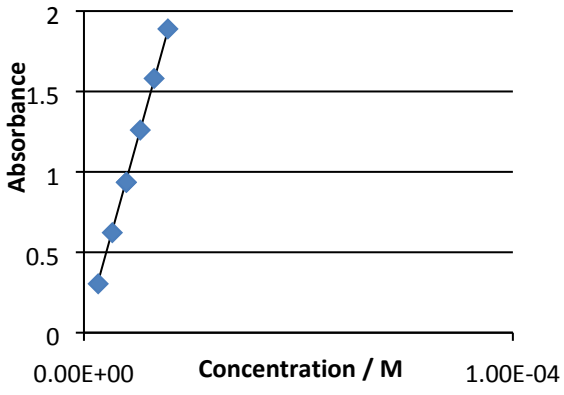

c)

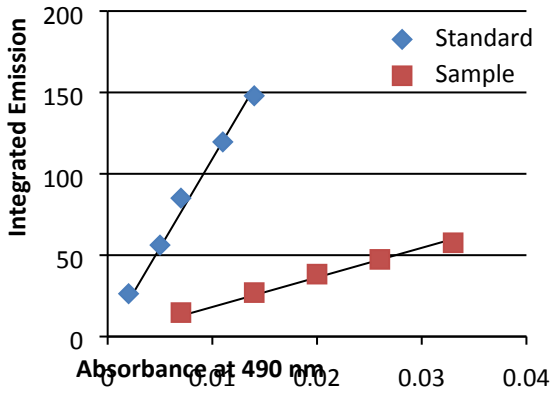

Figure S6. a) Normalized absorption and emission spectra of [**3**]OTf. **b)** Beer-Lambert absorbance plot. **c)** Quantum yield gradient plot.

a)

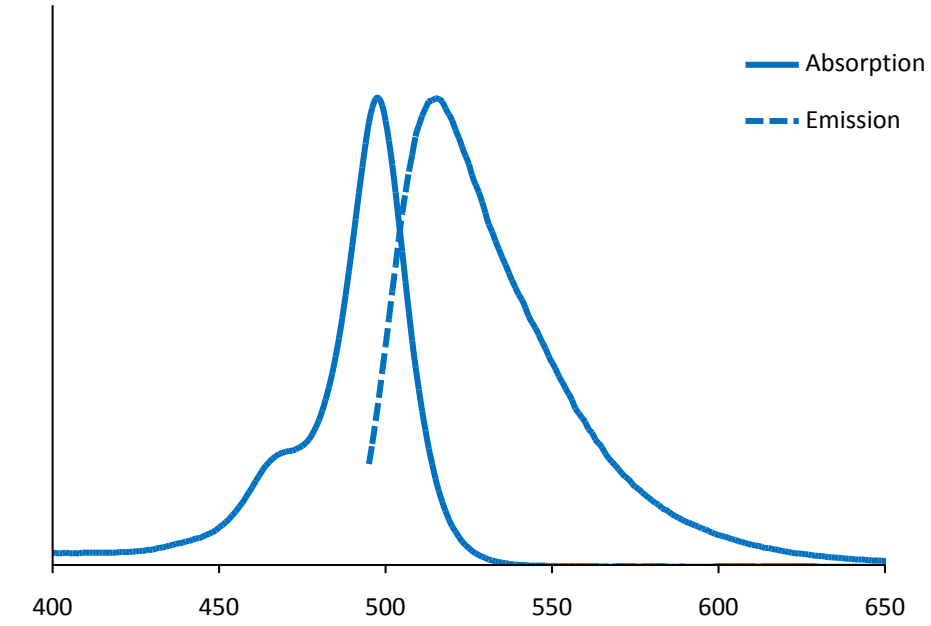

b)

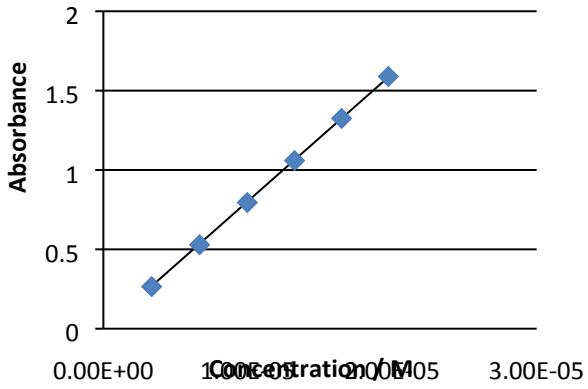

c)

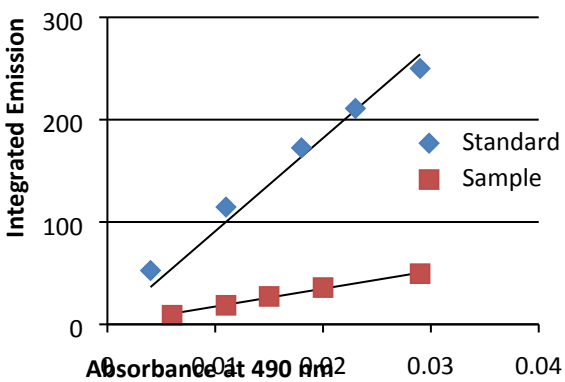

S5. NMR Spectra of Anion Binding to [3]OTf and $Ph_3SbMeOTf$.

Table S4. Summary of ^1H NMR chemical shifts corresponding to the Sb-bound methyl group of [**3**]OTf and $Ph_3SbMeOTf$ upon anion addition.

	$CDCl_3$		CD_3OD	
[**3**]OTf	Original	2.64 ppm	Original	2.56 ppm
	TBAF	2.41 ppm	KF	2.16 ppm
	TBACN	2.32 ppm	TBACN	2.20 ppm
	$TBAN_3$	2.33 ppm	$TBAN_3$	2.53 ppm
$Ph_3SbMeOTf$	Original	2.57 ppm		
	TBAF	1.99 ppm		
	TBACN	2.50 ppm		
	$TBAN_3$	2.40 ppm		

Figure S7. ^1H NMR spectral changes for [**3**]OTf upon addition of KF, TBACN, and $TBAN_3$ in CD_3OD.

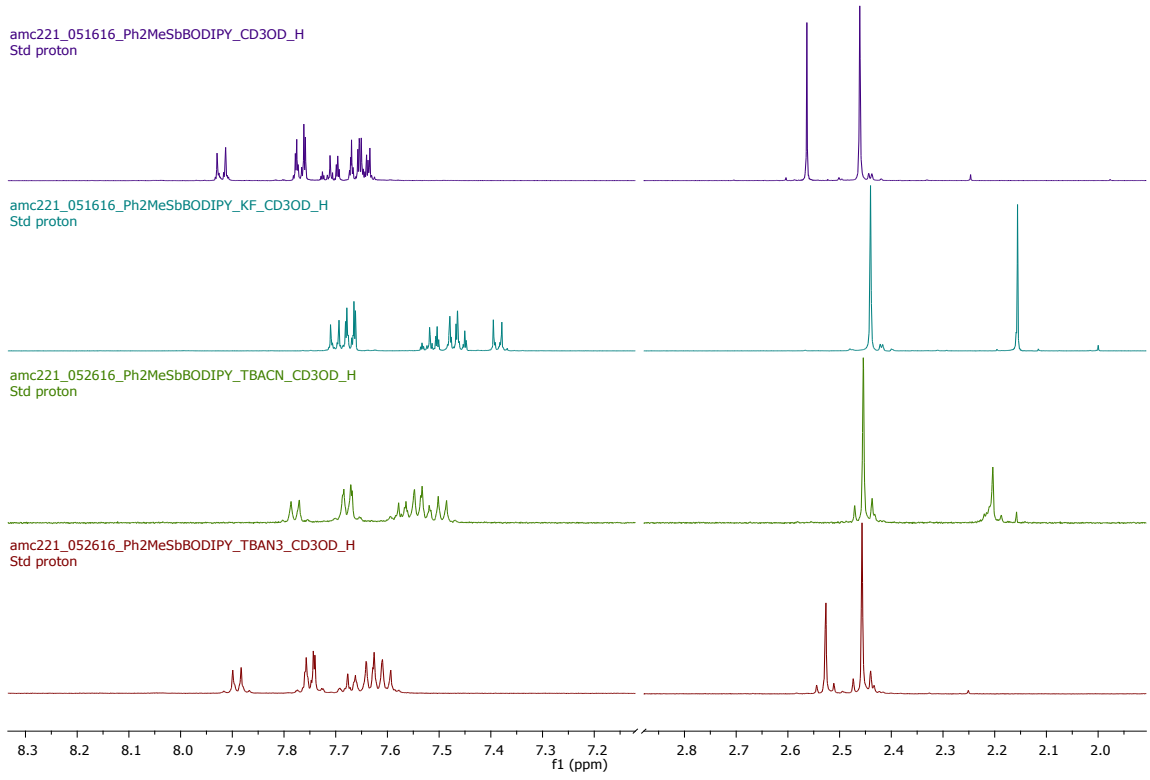

Figure S8. ^{1}H NMR spectral changes for [**3**]OTf upon addition of TBAF, TBACN, and $TBAN_3$ in $CDCl_3$.

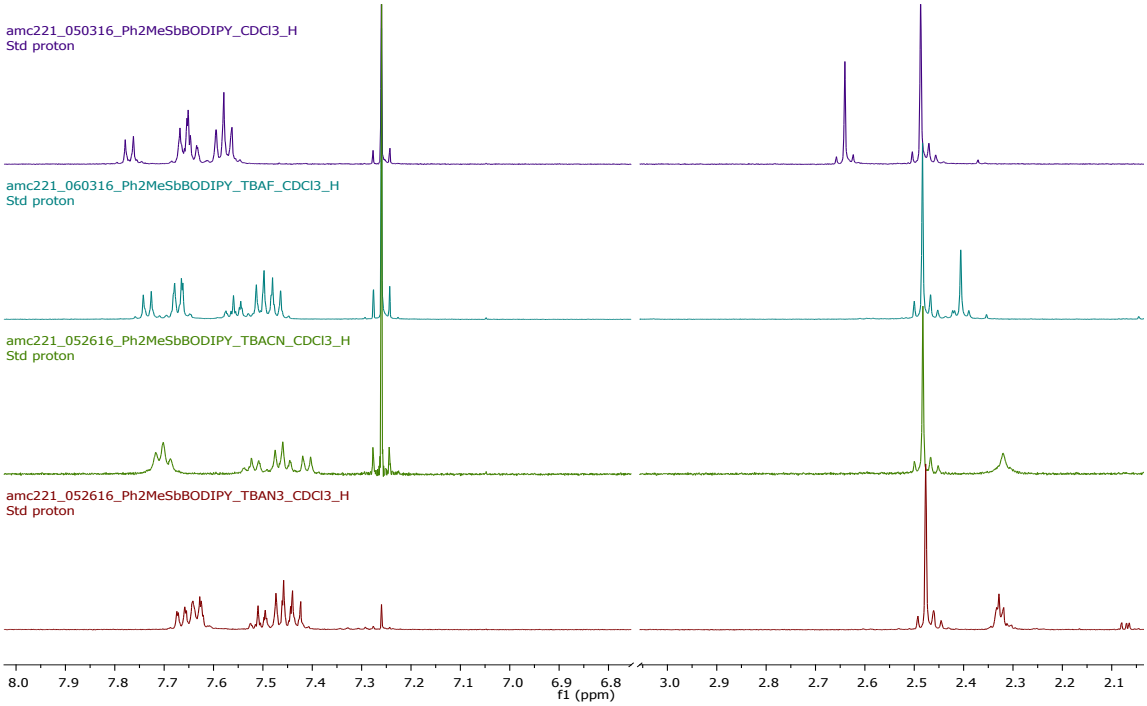

Figure S9. ^{1}H NMR spectral changes for $Ph_3SbMeOTf$ upon addition of TBAF, TBACN, and $TBAN_3$ in $CDCl_3$. The small signal at 2.17 ppm in the first two spectra is due to an acetone impurity.

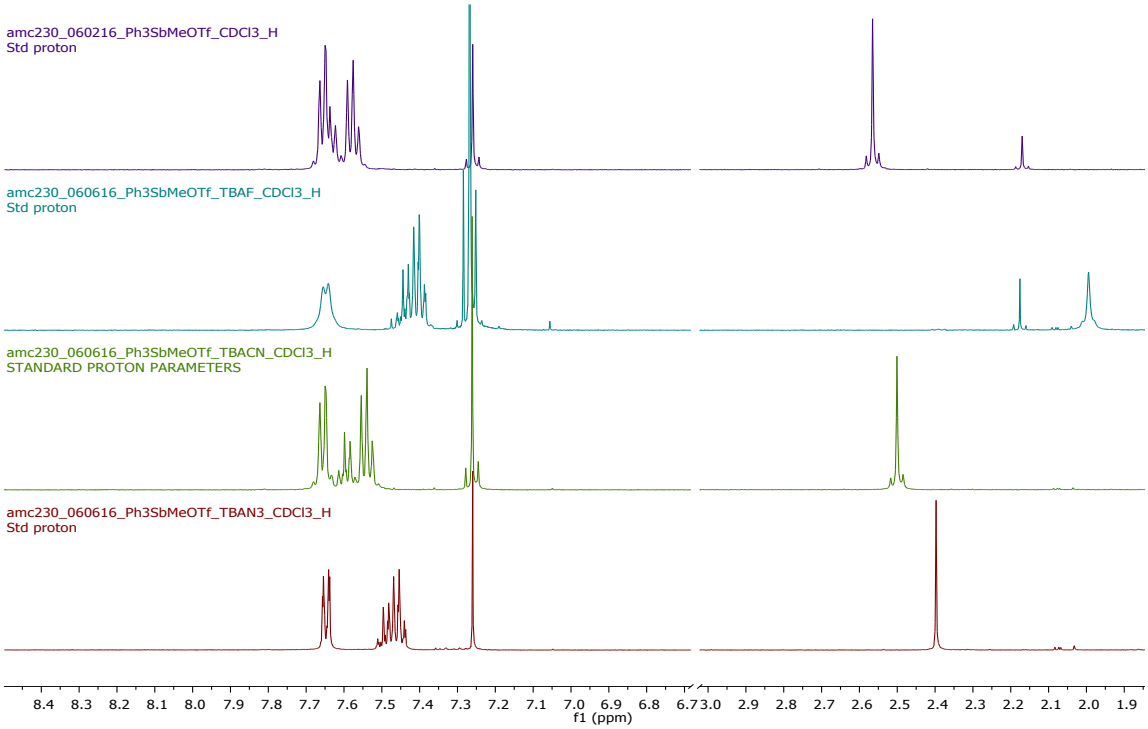

S6. Fluorescence Titration Data for Fluoride and Cyanide Binding to [3]OTf

Titrations were carried out in acetonitrile by addition of 10-µL aliquots of TBAF or TBACN stock solution to dilute 3.00-mL samples of [**3**]OTf. Emission spectra were obtained 3 minutes after mixing with λ_{exc} = 475 nm. The resulting spectra and titration curves for the binding of fluoride and cyanide to [**3**]OTf are shown as Figures S10 and S11 below. Binding constants (K_f) were calculated by fitting the data according to a known method.[7]

Limits of detection were calculated based on the titration data according to a literature method. [8-10] Fluorescence intensities were normalized between the minimum and maximum fluorescence intensity at 504 nm for [**3**]OTf treated with TBAF or TBACN and plotted against the log of concentration of added anion. These plots are shown as Figure S12 below. Linear regressions were fitted through the data, and the point at which this line crosses the ordinate axis for each was taken as the limit of detection for fluoride or cyanide by [**3**]OTf under these experimental conditions.

Figure S10. a) Emission spectra obtained upon titration of [**3**]OTf with TBAF. Concentration of [**3**]OTf = 2.00×10^{-6} M. Stock solution of TBAF = 1.22×10^{-4} M. b) Titration curve of emission at 504 nm with addition of TBAF.

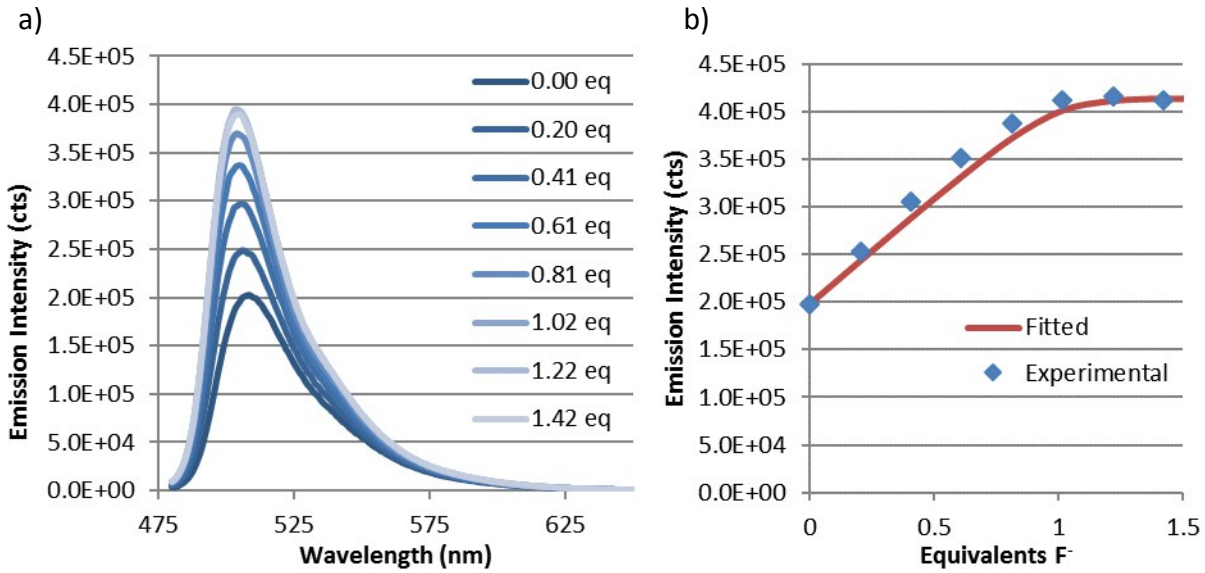

Figure S11. a) Emission spectra obtained upon titration of [**3**]OTf with TBACN. Concentration of [**3**]OTf = 1.93×10^{-6} M. Stock solution of TBACN = 1.10×10^{-4} M. b) Titration curve of emission at 504 nm with addition of TBACN.

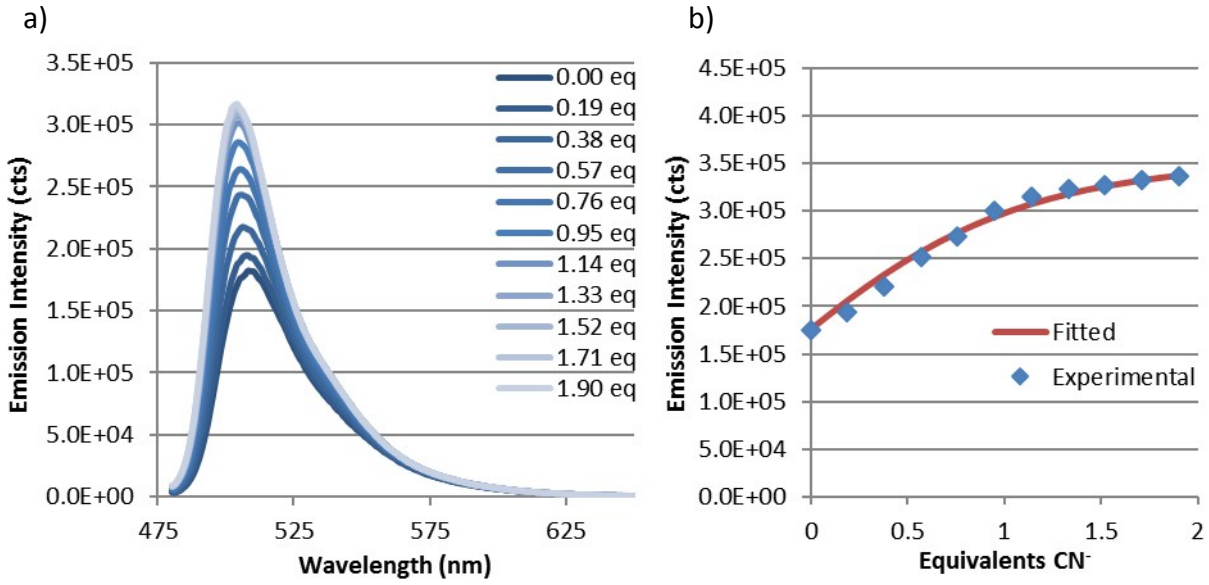

Figure S12. Linear regressions of normalized fluorescence intensities of [**3**]OTf titrated with a) TBAF, b) TBACN.

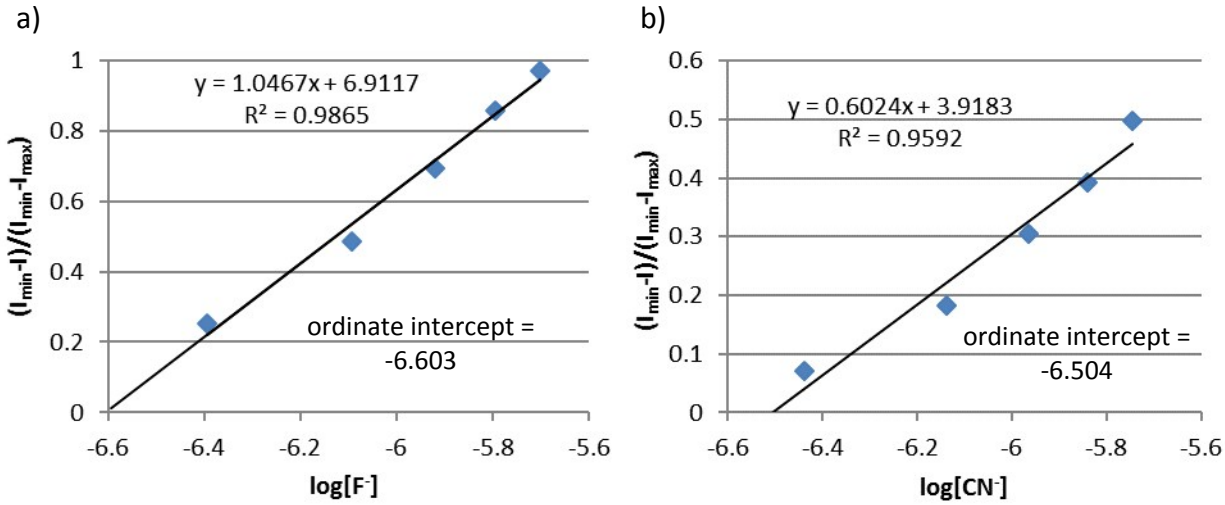

S7. DFT Optimization Results

Ground State Optimization Results.

DFT optimized structures for free [**3**]$^+$ and the fluoride- and cyanide-bound forms **3**-F and **3**-CN were first calculated in the gas phase (Figure S13). In the anion-bound forms of the molecule, the HOMO and LUMO are localized in the BODIPY π-π* system, as expected for an emissive molecule. However, in the free stibonium [**3**]$^+$, the LUMO is instead localized at the $SbPh_2Me$ fragment, with significant contribution from an Sb-Ph σ* orbital. TD-DFT calculations were performed on [**3**]$^+$ to determine the accessibility of this orbital in the excited state, which would be expected to result in a less emissive state than the expected π* orbital, resulting in the observed quenching of fluorescence in the free stibonium form.

Figure S13. Frontier molecular orbitals of S_0-optimized geometries of [**3**]$^+$, **3**-F and **3**-CN.

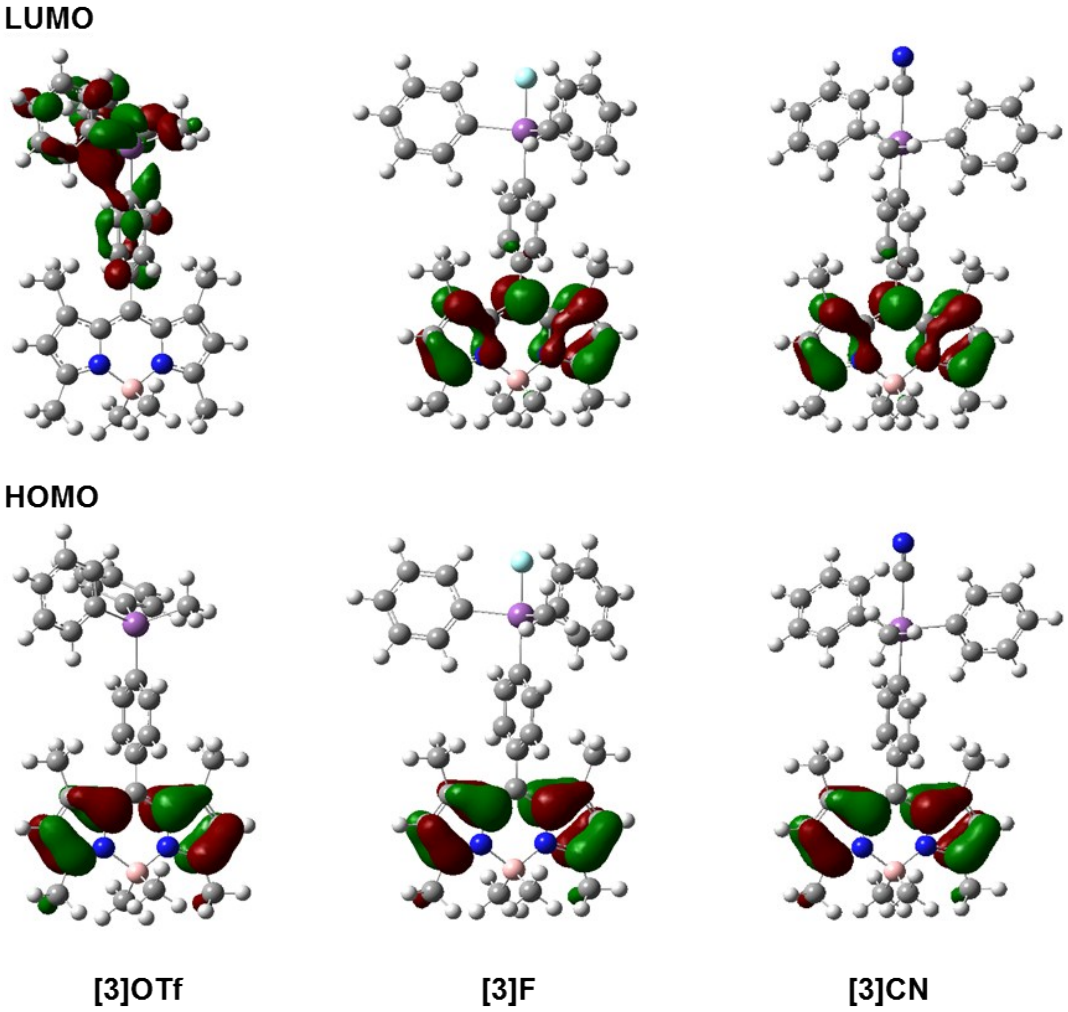

Excited State Optimization Procedure.

For the excited state optimizations of [**3**]$^+$, the following approach was taken. First, the ground state (S_0) geometry of [**3**]$^+$ was optimized, including the PCM solvent function for acetonitrile. The resulting S_0-optimized geometry was then used in a single-point TD-DFT calculation to determine the vertical excitation energy of electronic transitions to the first few singlet excited states. The first singlet excited state S_1 was confirmed to have primarily $\pi \rightarrow \pi^*$ character and to have significant oscillation strength, so this state was chosen for optimization. A TD-DFT geometry optimization of the excited state S_1 was then performed, starting from the S_0-optimized geometry. The resulting S_1-optimized geometry is shown in Figure S14 below as structure A. A second TD-DFT geometry optimization of the excited state S_1 was performed in which the initial geometry of the molecule was modified, distorting the geometry around Sb toward a more open, see-saw structure; this calculation yielded a different optimized geometry of comparable energy, which is shown in Figure S14 below as structure B.

Excited State Optimization Results.

Table S5. Energies calculated for the optimized ground and excited states of **[3]$^+$**.

	S_0 Optimized	S_1 Vertical Excitation	S_1 Optimized A	S_1 Optimized B
Energy (HF)	-1692.495	-1692.386	-1692.3998	-1692.3996
Relative Energy (eV)	0.00	2.96	2.58	2.59
HOMO-LUMO gap (eV)	3.11	N/A	2.63	1.03

Two optimized geometries for the first singlet excited state of [**3**]$^+$ were identified, shown as structures A and B in Figure S14. The energies of both S_1-optimized geometries A and B are very similar to each other, approximately 0.38 eV stabilized from the energy of S_1 upon vertical excitation, suggesting that both geometries may be accessible in the excited state. In geometry A, the substituents around Sb form a distorted tetrahedral arrangement with no prominent steric opening. The frontier molecular orbitals in this geometry are therefore localized in the π-π* system of the BODIPY fragment, making this state likely to be highly emissive. In geometry B, the substituents around Sb distort towards a see-saw structure with a prominent open site at Sb. The ground-state HOMO in this geometry is localized in the BODIPY π system, but the ground-state LUMO is localized in the Sb-R σ*-based orbital formed by the opening of the substituents around the Sb center. This state is likely to have low emission due to the removal of electrons from the BODIPY π-π* system. The HOMO-LUMO gap also shrinks dramatically in the case of structure B, increasing the likelihood of deactivation of the excited state in this geometry by radiationless internal conversion.[11, 12] The accessibility of this "dark" state after excitation would therefore partially quench the BODIPY emission in [**3**]$^+$. See main text for additional discussion.

Figure S14. Structures and frontier molecular orbitals of S_1-optimized geometries A and B. Bond distances displayed in angstroms (Å) and bond angles in degrees (°). Relative MO energies displayed in units of Hartrees.

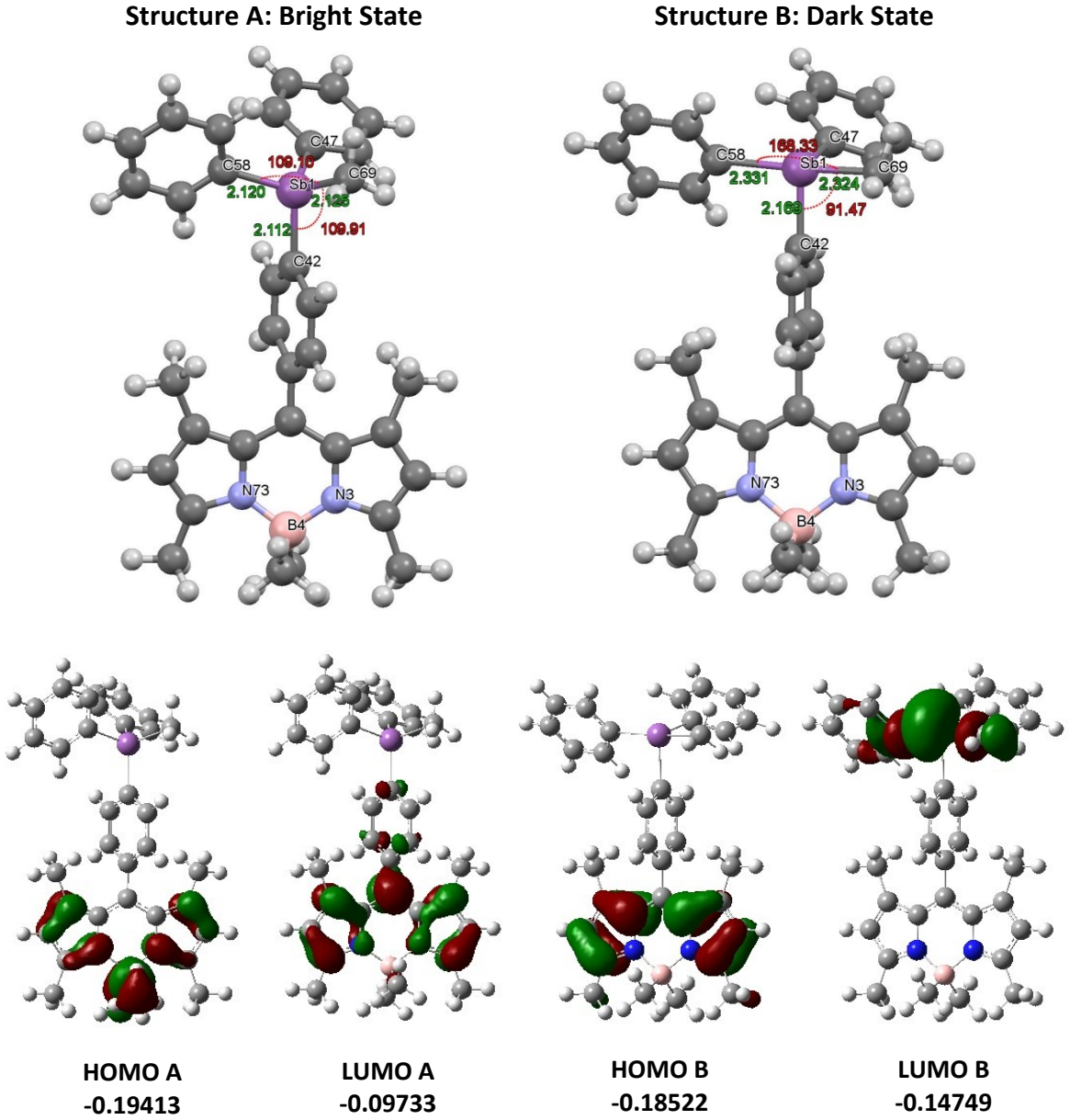

Table S6. Computationally determined xyz coordinates for all structures.

A. Gas-phase S_0-optimized geometry of $[3]^+$

Sb	-3.466713	-0.624226	-0.833893
C	5.587820	-2.270149	-0.343600
N	5.065876	-1.045165	-0.160058
B	5.852020	0.288779	0.226101
C	3.371104	-2.496204	-0.730839
C	3.674825	-1.139906	-0.386715
C	2.847696	-0.047283	-0.142290
C	3.339993	1.188983	0.281897
C	2.688312	2.436728	0.553724
C	3.695977	3.321355	0.882014
H	3.574446	4.235913	1.105855
C	4.916533	2.660366	0.833451
C	7.029441	-2.660611	-0.132712
H	7.233099	-3.455869	-0.669234
H	7.177399	-2.858272	0.814936
H	7.610674	-1.922288	-0.408420
C	2.058877	-3.157476	-1.034762
H	1.752381	-2.879078	-1.922451
H	1.397295	-2.894587	-0.362645
H	2.172975	-4.130752	-1.017752
C	1.241155	2.786386	0.476810
H	1.142672	3.760201	0.428504
H	0.780590	2.450590	1.274793
H	0.846775	2.377514	-0.322242
C	6.247140	3.278754	1.151870
H	6.943796	2.846931	0.614459
H	6.444460	3.156794	2.103706
H	6.219586	4.236100	0.944903
C	6.666369	0.060552	1.606939
H	7.174359	0.870546	1.824512
H	7.282106	-0.695095	1.502164
H	6.033778	-0.132206	2.330657
C	6.719740	0.726134	-1.092033
H	6.114049	1.068063	-1.782015
H	7.202728	-0.052757	-1.438229
H	7.361053	1.424811	-0.842915
C	1.373708	-0.219857	-0.294534
C	0.815512	-0.302625	-1.561542
H	1.375953	-0.267403	-2.328355
C	-0.555872	-0.435999	-1.718122
H	-0.933129	-0.478063	-2.588994

C	-1.377005	-0.510487	-0.597254
C	-0.815639	-0.451737	0.676309
H	-1.373092	-0.516628	1.442690
C	0.552262	-0.301690	0.827266
H	0.930623	-0.254072	1.696849
C	-4.218746	-1.373019	0.996969
C	-5.183063	-0.607168	1.641822
H	-5.513986	0.184615	1.234062
C	-5.661809	-1.004556	2.882858
H	-6.316471	-0.478455	3.326371
C	-5.194169	-2.154237	3.474575
H	-5.526957	-2.418228	4.324988
C	-4.242879	-2.926524	2.836999
H	-3.932863	-3.728595	3.241188
C	-3.732882	-2.525649	1.590702
H	-3.060888	-3.039175	1.159019
C	-4.004409	1.428195	-0.713232
C	-5.078488	1.962215	-1.413742
H	-5.571279	1.417550	-2.016025
C	-5.430258	3.291584	-1.234243
H	-6.156743	3.657469	-1.724371
C	-4.728390	4.090817	-0.345304
H	-4.985067	4.997247	-0.216867
C	-3.652636	3.569683	0.358143
H	-3.169742	4.118291	0.964113
C	-3.284342	2.244544	0.172264
H	-2.541070	1.889285	0.646471
C	-3.857574	-1.312345	-2.788549
H	-4.431036	-0.667112	-3.252302
H	-4.309936	-2.180490	-2.744081
H	-3.013057	-1.407869	-3.275636
N	4.727928	1.375561	0.469202
C	4.581887	-3.161183	-0.703902
H	4.708981	-4.081596	-0.901096

B. Gas-phase S_0-optimized geometry of [3]F

Sb	3.503149	-0.421734	-0.787844
F	5.590928	-0.399510	-0.964184
C	-4.974138	2.605050	0.860510
N	-5.130392	-1.059800	-0.238320
C	-3.731155	3.247361	0.913692
H	-3.595034	4.157446	1.147884
C	-2.738638	2.363410	0.573906
C	-3.410289	1.152765	0.273043

C	-2.922342	-0.082492	-0.179426
C	-3.744601	-1.162174	-0.465615
C	-3.452426	-2.508637	-0.814599
C	-4.663073	-3.168450	-0.808907
H	-4.791589	-4.084578	-1.025770
C	-5.661196	-2.285282	-0.438417
C	-6.288935	3.221897	1.152254
H	-6.492213	3.120504	2.105088
H	-6.982105	2.777378	0.620885
H	-6.259841	4.173446	0.922620
C	-1.279133	2.710972	0.548857
H	-0.844799	2.351762	1.350185
H	-1.174291	3.683532	0.527592
H	-0.865167	2.320608	-0.250899
C	-2.126435	-3.159537	-1.113498
H	-1.468860	-2.881179	-0.442952
H	-1.821379	-2.885813	-2.003831
H	-2.227989	-4.134488	-1.088886
C	-7.079877	-2.639906	-0.252713
H	-7.289308	-3.438985	-0.779412
H	-7.643944	-1.895851	-0.549269
H	-7.249873	-2.819513	0.696882
C	-6.768453	0.017334	1.531870
H	-7.563233	-0.515079	1.318918
H	-7.044799	0.876601	1.910342
H	-6.218149	-0.464491	2.183923
C	-6.764785	0.735617	-1.119205
H	-7.383679	0.020522	-1.374910
H	-6.154590	0.921700	-1.864759
H	-7.271851	1.544879	-0.902291
C	-1.432947	-0.250873	-0.320371
C	-0.625054	-0.378709	0.816904
H	-1.015227	-0.383970	1.684002
C	0.743909	-0.495977	0.666386
H	1.283070	-0.605329	1.441060
C	1.359533	-0.458757	-0.583710
C	0.521590	-0.323313	-1.688236
H	0.908341	-0.283406	-2.555962
C	-0.850063	-0.248306	-1.564475
H	-1.393440	-0.192387	-2.341125
C	3.923152	-1.451868	1.025027
C	4.791325	-0.866505	1.940055
H	5.198984	-0.031798	1.742394
C	5.061596	-1.500457	3.131268

H	5.649407	-1.096445	3.759549
C	4.477084	-2.726547	3.422397
H	4.659323	-3.159103	4.248779
C	3.634520	-3.316599	2.506375
H	3.258186	-4.168858	2.685517
C	3.337101	-2.658051	1.327208
H	2.722109	-3.046830	0.715664
C	3.738620	1.627940	-0.543681
C	2.843516	2.336421	0.292010
H	2.100719	1.878535	0.668447
C	3.024515	3.683063	0.574170
H	2.418727	4.137250	1.150679
C	4.085053	4.360124	0.017871
H	4.229168	5.275887	0.222405
C	4.950136	3.692180	-0.852853
H	5.651866	4.166508	-1.281301
C	4.785896	2.358014	-1.086951
H	5.412907	1.911631	-1.644109
C	3.627509	-1.289027	-2.681336
H	3.880205	-2.232193	-2.592965
H	4.302582	-0.819297	-3.213572
H	2.757280	-1.225372	-3.127549
N	-4.794390	1.338829	0.460641
B	-5.907213	0.270707	0.175869

C. Gas-phase S_0-optimized geometry of [3]CN

Sb	3.412155	-0.409716	-0.750293
C	-5.083675	2.598122	0.836108
N	-5.223123	-1.069324	-0.256303
C	-3.842749	3.243797	0.896168
H	-3.710550	4.154704	1.129408
C	-2.845713	2.361772	0.564711
C	-3.512206	1.148767	0.261887
C	-3.018067	-0.086111	-0.184860
C	-3.835603	-1.168518	-0.474266
C	-3.537623	-2.514908	-0.818594
C	-4.746554	-3.177882	-0.819532
H	-4.871248	-4.094777	-1.035381
C	-5.749397	-2.296594	-0.457407
C	-6.401970	3.212102	1.117945
H	-6.611254	3.112089	2.069624
H	-7.090463	2.764700	0.582927
H	-6.373848	4.163262	0.886581
C	-1.386986	2.713111	0.548563

H	-0.957004	2.356651	1.353458
H	-1.284546	3.685898	0.526020
H	-0.966746	2.322229	-0.247660
C	-2.207997	-3.162926	-1.107442
H	-1.555582	-2.881499	-0.433148
H	-1.897800	-2.890190	-1.996301
H	-2.307167	-4.138089	-1.081525
C	-7.168340	-2.654565	-0.280326
H	-7.372212	-3.455246	-0.806772
H	-7.732382	-1.912588	-0.582093
H	-7.344117	-2.832711	0.668493
C	-6.875612	0.007061	1.500885
H	-7.667581	-0.527862	1.283786
H	-7.156686	0.866358	1.875790
H	-6.328359	-0.472009	2.157519
C	-6.856360	0.720028	-1.151558
H	-7.471688	0.002799	-1.409881
H	-6.241756	0.906214	-1.893456
H	-7.366954	1.528390	-0.939624
C	-1.527342	-0.250867	-0.315660
C	-0.726625	-0.374299	0.827164
H	-1.122485	-0.378844	1.691684
C	0.643601	-0.488278	0.685895
H	1.177932	-0.594660	1.464320
C	1.267346	-0.451952	-0.560195
C	0.436344	-0.320924	-1.670483
H	0.828696	-0.281745	-2.535725
C	-0.936286	-0.249268	-1.555903
H	-1.474680	-0.196334	-2.336224
C	3.822897	-1.435103	1.067384
C	4.683494	-0.845629	1.986918
H	5.090266	-0.010254	1.790254
C	4.947568	-1.476477	3.181165
H	5.530172	-1.069665	3.812481
C	4.364354	-2.703510	3.470923
H	4.542275	-3.133926	4.299360
C	3.529384	-3.297608	2.550573
H	3.154104	-4.150489	2.728960
C	3.238019	-2.642210	1.368143
H	2.628085	-3.033828	0.753354
C	3.640663	1.641055	-0.508737
C	2.738228	2.348861	0.319610
H	1.994166	1.889785	0.692077
C	2.913849	3.696537	0.600228

H	2.303095	4.150289	1.171817
C	3.976258	4.375259	0.049549
H	4.116631	5.291807	0.253173
C	4.848796	3.707841	-0.814108
H	5.552093	4.183147	-1.238889
C	4.689585	2.372782	-1.046581
H	5.321414	1.926927	-1.598695
C	3.551246	-1.280480	-2.641166
H	3.805815	-2.222800	-2.549225
H	4.228581	-0.810049	-3.169898
H	2.683811	-1.220003	-3.093225
N	-4.897993	1.331577	0.439995
B	-6.006125	0.259969	0.150070
C	5.585391	-0.381264	-0.919508
N	6.728434	-0.366300	-1.008509

D. MeCN-solvated S_1-optimized geometry A of $[3]^+$ (Bright State)

Sb	-3.411280	-0.332915	-0.695188
C	5.557143	-2.310415	-0.556779
N	5.092115	-1.096042	-0.230924
B	5.948943	0.207017	0.108028
C	3.306669	-2.439342	-0.774854
C	3.695798	-1.129695	-0.352130
C	2.925205	-0.004900	-0.053971
C	3.493556	1.190816	0.387739
C	2.882893	2.425102	0.773939
C	3.922162	3.252351	1.145321
H	3.840095	4.272941	1.496665
C	5.133863	2.549784	0.989791
C	6.987202	-2.740706	-0.554448
H	7.090646	-3.638215	-1.169694
H	7.321864	-2.996177	0.456726
H	7.661087	-1.976178	-0.942561
C	1.947190	-3.006023	-1.045751
H	1.414437	-2.455032	-1.825869
H	1.311019	-2.999342	-0.155706
H	2.047460	-4.043519	-1.376681
C	1.439565	2.823582	0.804889
H	1.358037	3.862188	1.137393
H	0.853573	2.205621	1.491519
H	0.966416	2.747612	-0.178379
C	6.477098	3.119455	1.308155
H	7.242531	2.830237	0.587450
H	6.817807	2.801412	2.299538

H	6.408661	4.210332	1.320199
C	6.938370	-0.105559	1.355591
H	7.528176	0.767276	1.652173
H	7.665912	-0.889170	1.123110
H	6.387010	-0.436379	2.247089
C	6.673849	0.708786	-1.261456
H	5.941888	0.909120	-2.056402
H	7.379890	-0.028391	-1.663113
H	7.246415	1.633822	-1.121682
C	1.442539	-0.089097	-0.197809
C	0.839251	0.234411	-1.413353
H	1.450812	0.546384	-2.253894
C	-0.541082	0.157887	-1.552786
H	-0.994455	0.413384	-2.505757
C	-1.325815	-0.246309	-0.471589
C	-0.728382	-0.572257	0.745956
H	-1.328812	-0.892260	1.591595
C	0.653391	-0.492425	0.878845
H	1.120183	-0.745556	1.825394
C	-4.191440	-1.547068	0.829381
C	-5.130398	-1.032055	1.723740
H	-5.464569	-0.002231	1.646781
C	-5.643104	-1.849381	2.726675
H	-6.373180	-1.450420	3.423754
C	-5.220481	-3.170684	2.835040
H	-5.622296	-3.804714	3.619314
C	-4.283086	-3.682311	1.941527
H	-3.953000	-4.712759	2.026296
C	-3.764784	-2.873265	0.936096
H	-3.031755	-3.278887	0.244793
C	-4.204252	1.599570	-0.522422
C	-5.319022	1.958558	-1.282059
H	-5.775072	1.251278	-1.968534
C	-5.847778	3.239670	-1.159720
H	-6.713232	3.522603	-1.750427
C	-5.267898	4.152997	-0.284016
H	-5.682694	5.151966	-0.191965
C	-4.156659	3.791371	0.472869
H	-3.704387	4.504882	1.154285
C	-3.619922	2.513384	0.356913
H	-2.749197	2.238869	0.945158
C	-3.878294	-1.126705	-2.581816
H	-4.962385	-1.125816	-2.701444
H	-3.494742	-2.146927	-2.626271

H	-3.410687	-0.509969	-3.350227
N	4.882167	1.313409	0.537296
C	4.480136	-3.153976	-0.894944
H	4.576190	-4.189265	-1.196187

D. MeCN-solvated S_1-optimized geometry B of $[3]^+$ (Dark State)

Sb	-3.521054	-0.395921	-1.039989
C	5.386726	-2.408984	-0.059481
N	4.929059	-1.151667	0.023121
B	5.792156	0.181940	0.176635
C	3.148905	-2.551426	-0.376642
C	3.540796	-1.191901	-0.167940
C	2.777689	-0.024582	-0.113956
C	3.345282	1.224308	0.143273
C	2.739423	2.513187	0.273502
C	3.773566	3.382225	0.552179
H	3.693096	4.449450	0.714925
C	4.977726	2.651126	0.589361
C	6.805881	-2.846592	0.097561
H	6.924216	-3.839094	-0.344939
H	7.081381	-2.924215	1.154855
H	7.514326	-2.168790	-0.379870
C	1.794792	-3.143076	-0.619833
H	1.315157	-2.732036	-1.512501
H	1.112575	-2.974010	0.218582
H	1.892062	-4.223498	-0.758505
C	1.304577	2.925482	0.154027
H	1.226002	4.007062	0.295195
H	0.670987	2.443475	0.904227
H	0.882924	2.683125	-0.825630
C	6.313161	3.254196	0.877662
H	7.109900	2.835342	0.262243
H	6.594508	3.111401	1.926775
H	6.265684	4.330855	0.695359
C	6.707670	0.082933	1.512782
H	7.298007	0.988169	1.684821
H	7.430987	-0.736629	1.461495
H	6.103432	-0.080912	2.416153
C	6.598459	0.428519	-1.216877
H	5.913835	0.493755	-2.074101
H	7.310171	-0.374763	-1.443741
H	7.180900	1.357830	-1.208953
C	1.303454	-0.117689	-0.323232
C	0.771957	-0.006204	-1.608318

H	1.433326	0.147360	-2.454978
C	-0.600250	-0.092106	-1.808852
H	-0.997319	-0.003074	-2.815548
C	-1.449072	-0.292570	-0.719136
C	-0.923628	-0.405949	0.567940
H	-1.574212	-0.566719	1.421711
C	0.450501	-0.318027	0.761587
H	0.861320	-0.406054	1.762274
C	-4.138276	-1.334347	0.733598
C	-5.054837	-0.705358	1.576685
H	-5.455098	0.273276	1.331034
C	-5.459188	-1.340907	2.746935
H	-6.171745	-0.852902	3.404407
C	-4.951300	-2.594965	3.071859
H	-5.268710	-3.086912	3.986016
C	-4.036405	-3.220578	2.229065
H	-3.639814	-4.198517	2.482730
C	-3.626094	-2.593368	1.057602
H	-2.909896	-3.086557	0.406880
C	-3.953170	1.559629	-0.421718
C	-5.088358	2.204646	-0.915693
H	-5.745614	1.708576	-1.623871
C	-5.376770	3.499919	-0.497714
H	-6.257415	4.005036	-0.881552
C	-4.538303	4.143708	0.407724
H	-4.766095	5.154753	0.730857
C	-3.407498	3.497130	0.899250
H	-2.753611	4.000754	1.604104
C	-3.109868	2.202531	0.486620
H	-2.222991	1.705431	0.868555
C	-3.498077	-2.104538	-2.259608
H	-4.527744	-2.405011	-2.457775
H	-2.970188	-2.896356	-1.726406
H	-2.985704	-1.866068	-3.192388
N	4.726174	1.357114	0.346190
C	4.312756	-3.287804	-0.304641
H	4.404337	-4.360823	-0.414773

S8. References

1. B. A. Chalmers, M. Bühl, K. S. Athukorala Arachchige, A. M. Z. Slawin and P. Kilian, *Chem. Eur. J.*, 2015, **21**, 7520-7531.
2. L. Porrès, A. Holland, L.-O. Pålsson, A. Monkman, C. Kemp and A. Beeby, *J. Fluoresc.*, 2006, **16**, 267-273.
3. D. Magde, R. Wong and P. G. Seybold, *Photochem. Photobiol.*, 2002, **75**, 327-334.
4. L. Jiao, C. Yu, J. Li, Z. Wang, M. Wu and E. Hao, *J. Org. Chem.*, 2009, **74**, 7525-7528.
5. Gaussian 09, M. J. Frisch, G. W. Trucks, H. B. Schlegel, G. E. Scuseria, M. A. Robb, J. R. Cheeseman, G. Scalmani, V. Barone, B. Mennucci, G. A. Petersson, H. Nakatsuji, M. Caricato, X. Li, H. P. Hratchian, A. F. Izmaylov, J. Bloino, G. Zheng, J. L. Sonnenberg, M. Hada, M. Ehara, K. Toyota, R. Fukuda, J. Hasegawa, M. Ishida, T. Nakajima, Y. Honda, O. Kitao, H. Nakai, T. Vreven, J. A. Montgomery Jr., J. E. Peralta, F. Ogliaro, M. J. Bearpark, J. Heyd, E. N. Brothers, K. N. Kudin, V. N. Staroverov, R. Kobayashi, J. Normand, K. Raghavachari, A. P. Rendell, J. C. Burant, S. S. Iyengar, J. Tomasi, M. Cossi, N. Rega, N. J. Millam, M. Klene, J. E. Knox, J. B. Cross, V. Bakken, C. Adamo, J. Jaramillo, R. Gomperts, R. E. Stratmann, O. Yazyev, A. J. Austin, R. Cammi, C. Pomelli, J. W. Ochterski, R. L. Martin, K. Morokuma, V. G. Zakrzewski, G. A. Voth, P. Salvador, J. J. Dannenberg, S. Dapprich, A. D. Daniels, Ö. Farkas, J. B. Foresman, J. V. Ortiz, J. Cioslowski and D. J. Fox, Gaussian, Inc., Wallingford, CT, USA, 2009.
6. C. Würth, M. Grabolle, J. Pauli, M. Spieles and U. Resch-Genger, *Nat. Protocols*, 2013, **8**, 1535-1550.
7. I.-S. Ke, M. Myahkostupov, F. N. Castellano and F. P. Gabbaï, *J. Am. Chem. Soc.*, 2012, **134**, 15309-15311.
8. M. Shortreed, R. Kopelman, M. Kuhn and B. Hoyland, *Anal. Chem.*, 1996, **68**, 1414-1418.
9. A. Caballero, R. Martínez, V. Lloveras, I. Ratera, J. Vidal-Gancedo, K. Wurst, A. Tárraga, P. Molina and J. Veciana, *J. Am. Chem. Soc.*, 2005, **127**, 15666-15667.
10. J. Wang, W. Lin, L. Yuan, J. Song and W. Gao, *Chem. Commun.*, 2011, **47**, 12506-12508.
11. Z. Shuai, D. Wang, Q. Peng and H. Geng, *Acc. Chem. Res.*, 2014, **47**, 3301-3309.
12. M. Casalboni, F. De Matteis, P. Prosposito, A. Quatela and F. Sarcinelli, *Chem. Phys. Lett.*, 2003, **373**, 372-378.